# DUAL MESH APPROACH FOR SEMICONDUCTOR DEVICE SIMULATOR

T.Kojima, Y.Saito, and R.Dang

College of Engineering, Hosei University
3-7-2 Kajino-cho Koganei, Tokyo 184, Japan

Abstract : This paper describes a new discretization approach for 2-dimensional simulation of semiconductor devices. The approach essentially makes use of two interlaced dual mesh systems based on Delaunay triangles and associated Voronoi polygons, respectively. This discretization method is applied to the solution of Poisson's equation for a reverse-biased P-N junction. Potential, field and carrier distributions as well as junction capacitances are obtained which not only show a good agreement with conventional methods but also a promising prospective for improvement of simulation cost performance.

## INTRODUCTION

For analyzing semiconductor devices, numerical simulation techniques have been applied for quite some time. Although simulation methods are improved and accordingly device simulators are modified year by year, it still remains to fetch for a decisively reliable approach in terms of convergency and simulation turn-around time. The central difficulty of the problem lies in the fact that the device structures under simulation are very complicated and the governing fundamental equations are strongly nonlinear.

Recently, a new discretization method is proposed to the field problems [1], [2]. It makes use of a dual energy finite element approach which solves the dual energy functionals. To implement this method, two geometrically dual mesh systems, one made of the Delaunay triangles and the other of associated Voronoi polygons, have been introduced. And by utilizing the characteristics that simulated results involving functionals and local values converge to upper and lower limit with increasing mesh numbers, it has been pointed out that correct solutions can be found by composing results obtained with the two dual mesh systems [3], [4].

In this paper, we try applying this method to solve the semiconductor Poisson's equation. As an initial test example, we analyze a reverse-biased P-N junction problem. It is found that the new method is effective for wide areas. So this suggests that simulations of semiconductor devices may be carried out with a lower computational cost.

## VORONOI-DELAUNAY DISCRETIZATIONS

### Basic equations

For simplicity, a reverse-biased P-N junction is considered. In this case, the reverse current is almost negligible. The only governing equation is, thus, the following Poisson's equation.

$$\varepsilon \nabla^2 \psi = -q\,(p - n + N_D - N_A) = -\rho, \qquad (1)$$

where $\varepsilon$, $\psi$, $q$, $N_D$ and $N_A$ are the permitivity, potential, electron charge, donor and acceptor concentrations, respectively and $\rho$ is total charge densities. Also, $p$ and $n$ in (1) are the hole and electron densities given by

$$p = n_i \exp\left[\frac{q}{kT}(\phi_p - \psi)\right], \qquad (2)$$

$$n = n_i \exp\left[\frac{q}{kT}(\psi - \phi_n)\right], \qquad (3)$$

where $n_i$, $k$, $T$ are the intrinsic carrier concentration, Boltzmann constant, temperature, $\phi_p$ and $\phi_n$ are the quasi-Fermi levels of hole and electron, respectively. Since we are concerened only with a reverse-biased junction, it is legitimate for the time being to neglect minority carriers in each of the two semiconductor regions, namely $p$ in the N region and $n$ in the P region.

### Voronoi-Delaunay diagram

Delaunay triangulation of an arbitrary set of points is constructed by considering the geometrical duality with the set of Voronoi polygons. The circumcenters of Delaunay triangles are the vertices of the Voronoi polygons. Fig.1 shows the triangles in a Delaunay mesh. The Voronoi polygons associated with these Delaunay triangles are shown by dashed lines in this figure. By considering Fig.1, it is obvious that the Delaunay triangles and Voronoi polygons are locally orthogonal : each triangle side is perpendicular to the corresponding Voronoi polygon side. Furthermore, two complete but independent sets of nodal potential may be defined on this Voronoi-Delaunay diagram : one is located at the vertices of the Delaunay triangles ; and the other at the vertices of the Voronoi polygons. Thus, the governing equation (1) may be discretized either by the Delaunay or the Voronoi mesh system.

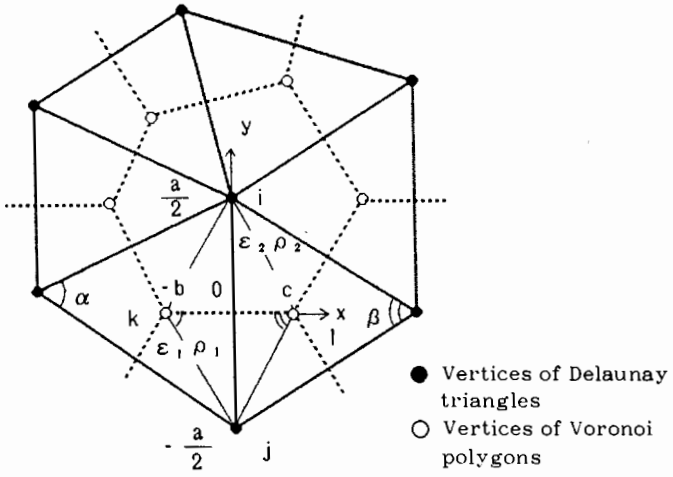


Fig.1. Voronoi-Delaunay diagram and locally orthogonal coordinate.

### Locally orthogonal discretizations

Equation (1) can be transformed into a boundary integral equation by application of Gauss' theorem as follows.

0018-9464/89/0700-2953$01.00©1989 IEEE

$$\int_l \varepsilon \frac{\partial \psi}{\partial n}\, dl + \int_s \rho\, dS = 0 . \qquad (4)$$

On the local coordinate system shown in Fig.1, nodes i and j are located on the boundary between the regions 1 and 2, where it is assumed that each of the Delaunay triangles takes a distinct permitivity $\varepsilon$. This means that a field intensity $E_y(=-\partial\psi/\partial y)$ in the direction of y-axis is common to both regions 1 and 2 in Fig.1. A simple Lagrange interpolation between the nodes i and j in Fig.1 yields a trial function for the Delaunay system as

$$\psi_e=(1/2)(\psi_i+\psi_j)+(\psi_i-\psi_j)(y/a) , \qquad (5)$$

where 'a' is the distance between the nodes i and j. Integrating over a portion of the Voronoi polygon enclosing node i after substituting (5) into (4) yields

$$\int_{-b}^{c} \varepsilon \frac{\partial \psi}{\partial y}\Big|_e dx + \int_{-b}^{c}\int_{0}^{a/2} \rho\, dx\, dy,$$

$$= -(1/2)(\varepsilon_1 \cot\alpha + \varepsilon_2 \cot\beta)(\psi_i-\psi_j)$$

$$+ (a/4)(b\rho_1 + c\rho_2) = 0. \qquad (6)$$

when (6) is applied to the other portions of Voronoi polygon enclosing node i, one obtains the full set of Delaunay nodal equations which satisfies the common tangential field strength between the adjacent Delaunay triangles.

On the other side, nodes k and l are located on the x-axis in Fig.1. In this case, flux density $D_x(=-\varepsilon\,\partial\psi/\partial x)$ must be continuous from region 1 to region 2. This boundary condition can be satisfied by selecting the following trial functions:

$$\psi_e=\{(\varepsilon_1\psi_k/b)+(\varepsilon_2\psi_i/c)+[\varepsilon_2(\psi_i-\psi_k)x/bc]\}$$

$$/\{(\varepsilon_1/b)+(\varepsilon_2/c)\}, -b \leqq x \leqq 0, \qquad (7a)$$

$$\psi_e=\{(\varepsilon_1\psi_k/b)+(\varepsilon_2\psi_i/c)+[\varepsilon_1(\psi_i-\psi_k)x/bc]\}$$

$$/\{(\varepsilon_1/b)+(\varepsilon_2/c)\}, 0 \leqq x \leqq c, \qquad (7b)$$

where the distances b, c are shown in Fig.1. Integrating over the portion of the Delaunay triangle enclosing node k after substituting (7a) into (4) yields

$$\int_{-a/2}^{a/2} \varepsilon \frac{\partial \psi}{\partial x}\Big|_e dy + \int_{-a/2}^{a/2}\int_{b}^{c} \rho\, dy\, dx$$

$$= -[2/\{(\cot\alpha/\varepsilon_1)+(\cot\beta/\varepsilon_2)\}](\psi_k-\psi_i)$$

$$+ (1/2)ab\rho_1 = 0 . \qquad (8)$$

Applying (8) to the other portions of the Delaunay triangle enclosing node k, the equations of Voronoi system are completed, which satisfies the continuity condition of normal flux density between the neighboring Delaunay triangles.

Duality

By means of (6) and (8), it is possible to derive the equivalent circuits of the Delaunay and Voronoi systems. Fig.2(a) and 2(b) show the equivalent circuits of the Delaunay and Voronoi systems, respectively. The parameters depending on the geometry and medium constant are obviously equivalent to the capacitances per unit length in these figures. By considering Fig.2(a), it is observed that the equivalent capacitances are connected in parallel to satisfy the common tangential field intensity condition between the adjacent Delaunay triangles. On the contrary, in Fig.2(b), the equivalent capacitances are connected in series to satisfy the normal flux density condition between the adjacent Delaunay triangles. Thus, the Voronoi-Delaunay discretizations form a dual relationship [5]. Furthermore, the inverse circuit relationship is established between Voronoi and Delaunay system.

$$1/2(\cot\alpha+\cot\beta)\cdot[2/(\cot\alpha+\cot\beta)] = 1 . \qquad (9)$$

Equation (9) reveals the geometrical duality in the Voronoi-Delaunay discretizations.

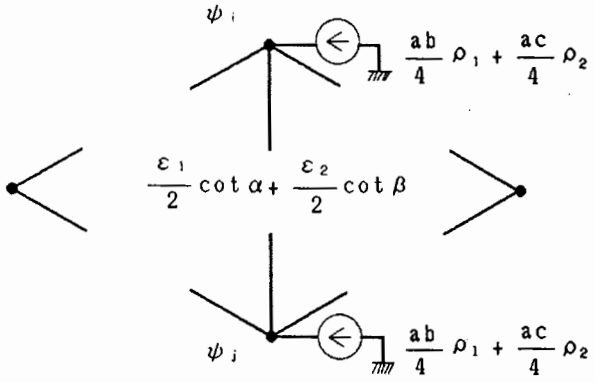


Fig.2(a). Equivalent circuit of Delaunay system,

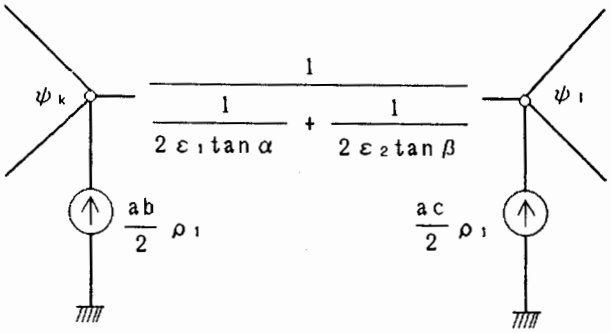


Fig.2(b). Equivalent circuit of Voronoi system,

This also suggests that the convergence of the numerical solutions may be accelerated by averaging the approximate solutions by (6) and (8).

For example, the midpoint potential $\psi_m$ in Fig.2(c) is given by

$$\psi_m = 1/2(\psi_i + \psi_k) . \qquad (10)$$

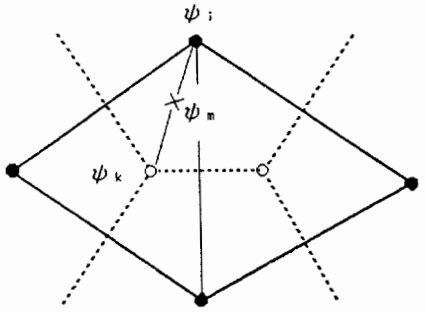


Fig.2(c) Location of an averaged potential $\psi_m$

An example

Figure 3 shows a simplified P-N junction model used as an initial test example. Various constants used in the computations are listed in Table 1. The iterative solution process was carried out by means of the Gummel algorithm [6].

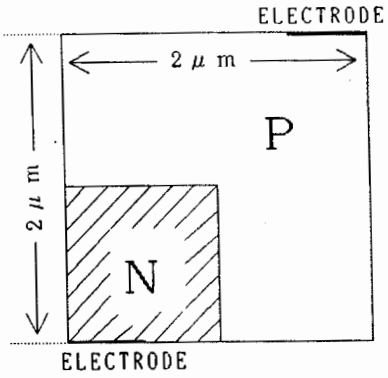


Fig.3. A simplified P-N junction model used as an initial test example.

Fig.4 and 5 shows the potential distributions and junction capacitance characteristics under different reverse-biased conditions. The results in Figure 4 reveal that averaging potentials by (10) yields better results even if a small number of nodes is employed.

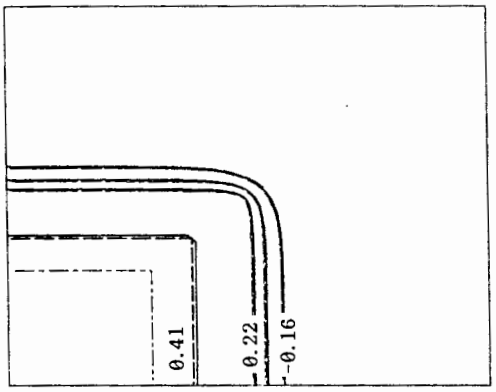


(a) ZERO BIASED

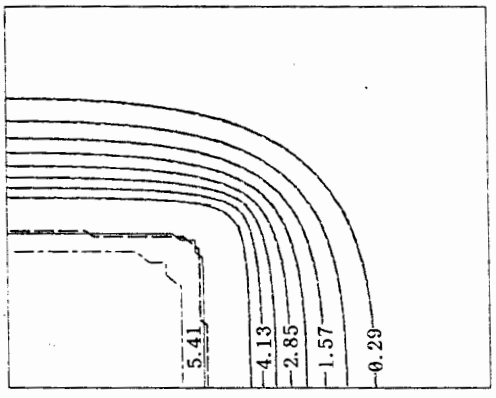


(b) 5V REVERESE- BIASED

FIG.4. Potential distributions under the different reverse-biased conditions.

Thus, our initial test example suggests that the simulation of semiconductor devices can be carried out in a more efficient manner using this Voronoi-Delaunay discretization method.

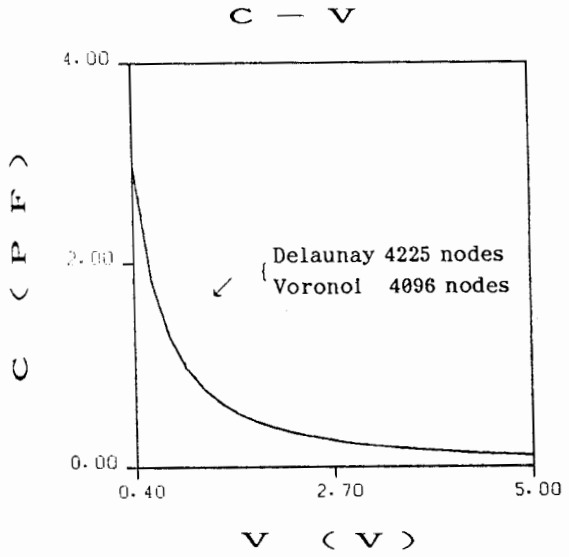


Fig.5. Capacitances between the electrodes under the different reverse-biased conditions.

## CONCLUSION

As shown above, we have proposed to utilize the Voronoi-Delaunay discretization method for the simulation of semiconductor devices. A simple example has demonstrated its versatility, and suggested that the simulation of semiconductor device may be carried out with a low computational cost.

## REFERENCES

[1] J.Penman, et al., "Complementary and dual energy finite element principles in magneto statics," IEEE Trans., Magn., MAG-18, 319 (1982).

[2] P.Hammond, et al., "Dual finite element calculations for static electric and magnetic fields," Proc.IEE, PT.A, Vol. 130, No.3, 105 (1983).

[3] Y.Saito, et al., "Faster magnetic field computation using locally orthogonal discretization," IEEE Trans., Magn., MAG-22, 1057 (1986).

[4] Y.Saito, et al., "Modeling of magnetization characteristics and faster magneto dynamic field computation," J. Appl.Phys.63(8), 3174 (1988).

[5] I.Vago, Graph Theory, Application to the Calculation of electrical networks, Elsvier Science Publishers, Amsterdam, The Netherlands (1985).

[6] H.K.Gummel, "A self-consistent iterative scheme for one dimensional steady-state transistor calculations," IEEE Trans., Electron Devices, Vol.ED-11, 455 (1964).

Table 1. Various constants used in the computers

| Parameter | Value | Units |
|---|---|---|
| $\varepsilon$ | 1.03e-12 | F/cm |
| q | 1.60e-19 | C |
| $N_D$ | 1.00e+16 | atoms/cm$^3$ |
| $N_A$ | 1.00e+17 | atoms/cm$^3$ |
| $n_i$ | 1.42e+10 | carriers/cm$^3$ |
| k T / q | 0.025 | V |